Pak. J. Bot., 44(3): 973-980, 2012.

CLONING, CHARACTERIZATION AND EXPRESSION OF ALLENE OXIDE CYCLASE GENE INVOLVED IN JASMONATE BIOSYNTHESIS FROM *TORENIA FOURNIERI*

YAN LIU[†], XIAO-MEI ZHAO[†], YAN HUANG, RU-YAN SUN AND JIN-HUA BIN[*]

Guangdong Provincial Key Laboratory of Biotechnology for Plant Development, College of Life Science, South China Normal University, Guangzhou 510631, The People's Republic of China
[*] *Corresponding author. Tel.:+86-20-8521-1372; E-mail: binjh@scnu.edu.cn*
[†] *These authors contributed equally to this work*

Abstract

Jasmonates are phytohormones that play important roles in plant defense and development. Allene oxide cyclase (AOC; EC 5.3.99.6) catalyzes a crucial step in the jasmonic acid biosynthetic pathway that forms the stereoisomeric precursor *cis*-(+)-12-oxophytodienoic acid. In the present study, a full-length cDNA of AOC was isolated from *Torenia fournieri* Lind., designated as *TfAOC* (GenBank accession no. JF417978). The cDNA was 954 bp in length. The 723 bp open reading frame encoded a protein of 240 amino acids with a putative chloroplast targeting sequence. The predicted molecular mass and the isoelectric point of the protein were 26.16 kDa and 8.60, respectively. Phylogenetic analysis reveals that TfAOC belongs to the AOC superfamily and is highly homologous to AOC proteins from other plant species. RT-PCR analysis revealed that *TfAOC* mRNA was expressed in all organs of plants, with highest expression in leaves and lowest in roots. High expression level was also detected in pistils and anthers. The level of methyl jasmonate was correlated with the expression of *TfAOC* mRNA. These results suggest that JA is involved in the pistil and anther development in *T. fournieri*.

Introduction

Jasmonic acid (JA) and methyl jasmonate (MeJA), along with their intermediate compounds collectively termed jasmonates (JAs), are ubiquitously occurring lipid-derived moleculars (Avanci *et al.*, 2010). Originally identified as a major component of fragrant oils, they have been shown to be a class of phytohormones with functions in plant defense and stress responses as well as plant development, especially reproduction (Feys *et al.*, 1994; McConn & Browse, 1996; Ishiguro *et al.*, 2001; Li *et al.*, 2001, 2004; Wasternack, 2007; Browse, 2009).

JA is produced from linolenic acid (α-LA, 18:3) released from chloroplast membranes through the octadecanoid pathway. Firstly, LA is catalyzed by 13-lipoxygenase (LOX) to form 13-hydroperoxy-9,11,15-octadecatrienoic acid (13-HPOT). Conversion of 13-HPOT is performed by allene oxide synthase (AOS), leading to an unstable allene oxide. Subsequently, allene oxide is converted to *cis*-(+)-12-oxophytodienoic acid (OPDA) by the enzyme allene oxide cyclase (AOC). For the final steps in JA production, the 12-OPDA molecule undergoes three cycles of β-oxidation inside the peroxisome (Avanci *et al.*, 2010). Obviously, OPDA is the stereoisomeric precursor of JA biosynthesis and the final product of the pathway of JA biosynthesis of the plastid-located part, AOC is therefore considered to be crucial in the JA biosynthetic pathway (Ziegler *et al.*, 2000; Hofmann *et al.*, 2006; Wasternack, 2007). The full-length cDNA coding for AOC was isolated first from tomato (Ziegler *et al.*, 2000). It was found that the content of JA and its amino acid conjugates were tightly correlated with the transcript levels of *AOC* (Hause *et al.*, 2003b). Afterwards, *AOC* cDNAs were also isolated and identified from *Arabidopsis* (Stenzel *et al.*, 2003b), barley (Maucher *et al.*, 2004), *Humulus lupulus* (Forts *et al.*, 2005) and *Hyoscyamus niger* (Jiang *et al.*, 2008), revealing that a signal peptide exists in the N terminus and *AOC* is expressed in most plant tissues. We are interested in cloning and characterization of *AOC* cDNA from *Torenia fournieri*, as *T. fournieri* is one of the most important ornamental species in Scrophulariaceae, which has unique and beautiful purple flowers (Aida *et al.*, 2000). It has naked embryo sacs that protrude from the micropyle in the four-nucleate stage and is a good model plant for studying pollen tube guidance and female development and fertilization events (Higashiyama *et al.*, 1998; Imre & Kristof, 1999; Higashiyama *et al.*, 2003).

In the present study, the full-length *AOC* cDNA was cloned from *T. fournieri* and the deduced AOC protein was characterized by phylogenetic analysis and other bioinformatic tools. The tissue-specific pattern of the *AOC* expression and the level of MeJA were investigated. The results suggest that JA is involved in anther and pistil development.

Materials and Methods

Plant materials and culture conditions: *Torenia fournieri* plants were grown from seeds in a controlled chamber at 25 ± 2°C. A photoperiod of 16/8 h (light/dark) cycles was achieved with cool and warm fluorescent lamps and the light intensity was about 50μmol photons m^{-2} s^{-1}.

Cloning of the full-length cDNA of *AOC*: Total RNA was extracted from leaves using the RNAiso Reagent (TaKaRa) following the manufacturer's instructions. The *AOC* cDNA was synthesized with the TaKaRa PrimeScript™ 1st Stand cDNA Synthesis Kit following the manufacturer's guidelines. For 3′ rapid amplification of cDNA ends (RACE), two degenerate primers, TfAOC3-1 and TfAOC3-2, were designed according to the conserved regions of other *AOC* gene sequences deposited in GenBank. The nucleotide sequences of the 3′ regions of *AOC* clones were obtained by nested RACE-PCR. The specific primers TfAOC5-1 and TfAOC5-2 were designed based on the 3′-RACE product and 5′ regions of *AOC* clones were obtained by RACE-PCR with the 5′-Full RACE Core Set (TaKaRa). Alignment and assemblage of the products of 3′-RACE and 5′-RACE enabled the full-length *AOC* to be deduced. Subsequently, the primers TfAOCfull5 and TfAOCfull3 were designed to amplify the open reading frame (ORF) of *AOC*. The amplified PCR products were purified and cloned into the PMD 18-T vector (TaKaRa), and the sequences were verified by DNA sequencing. All primers used in RACE are listed in Table 1.

Table 1. Primers used in the study.

Name	Purpose	Sequence
AP	cDNA	5'-GACTCGAGTCGACATCGATTTTTTTTTTTTTTTT-3'
AUAP	3' RACE	5'-GACTCGAGTCGCATCG-3'
TfAOC3-1	3' RACE	5'-CTCGG(A/C)GATCT(T/C)GT(G/C)CC-3'
TfAOC3-2	3' RACE	5'-AGCTT(T/C)TA(T/C)TTCGG(A/T/C)G(A/G)(T/C)TA(T/C)GG-3'
TfAOC5-1	5' RACE	5'-TTGACTCACAGCTCGCATCGCAATC-3'
TfAOC5-2	5' RACE	5'-AGAAGCTGTATATTGCCTCGTAACGG-3'
TfAOC full5	ORF	5'-ATGGCGGCTTCATCAGCATCTAC-3'
TfAOC full3	ORF	5'-TCAATCAGTAAAGCCCGGTAGAG-3'
TfGAPDH F1	RT-PCR	5'-ATGTTTGTTGTGGGTGTCA-3'
TfGAPDH R1	RT-PCR	5'-GTGAGGTCCACTACGGAGA-3'

Cloning of the genomic sequence of *AOC*: Total genomic DNA was extracted from *T. fournieri* leaves with the sodium dodecyl sulfate (SDS) method. The genomic DNA extract was used as a template in PCR amplification with the primers AOCfull5 and AOCfull3 to investigate the presence of introns. The amplification reactions were performed with the following protocol: 94°C for 3 min; 36 cycles of 94°C for 30 s, 55°C for 30 s, and 72°C for 1 min; and 72°C for 10 min. The PCR product was cloned into the PMD 18-T vector and sequenced.

Bioinformatic analysis: Molecular information for the TfAOC protein was obtained from the National Center of Biotechnological Information (NCBI) databases (http://www.ncbi.nlm.nih.gov). The nucleotide sequence, deduced amino acid sequence and ORF were analyzed and the sequence comparison was conducted using the protein blast program. The theoretical isoelectric point (pI) and molecular weight (Mw) of the protein were deduced with the Compute pI/Mw Tool (http://www.expasy.org/) (Bjellqvist *et al.*, 1993). Chloroplast transit peptide (cTP) analysis was carried out with the ChloroP 1.1 program (http://www.cbs.dtu.dk/services/Chlorop/) (Emanuelsson *et al.*, 1999) and TargetP 1.1 program online (http://www.cbs.dtu.dk/services/TargetP) (Emanuelsson *et al.*, 2000). Secondary structure prediction was performed with SOPMA (http://npsa-pbil.ibcp.fr/cgi-bin/npsa_automat.pl?page=npsa_sopma.html) (Combet *et al.*, 2000). Homology-based structural modeling was performed using Swiss-Model (http://swissmodel.expasy.org/) (Arnold *et al.*, 2006). Multiple alignment of amino acid sequences was achieved with DNAMAN 6.0 (Lynnon Biosoft, USA). A phylogenetic tree was constructed using the neighbor-joining method with MEGA 5.0 (Saitou & Nei, 1987).

RT-PCR: Total RNA was isolated from different organs (leaves, stems, roots and flowers) and tissues (anthers and pistils). All RNA samples were digested with DNase I (RNase-free) prior to use. Aliquots of 500 ng total RNA were employed in the reverse transcription reaction using random hexamer primers for the synthesis of first-strand cDNA. With TfAOCfull3 and TfAOCfull5 as primers, the amplification reactions were performed with the following protocol: denaturation at 94°C for 3 min; 28 cycles of 94°C for 30 s, 56°C for 30 s, and 72°C for 1 min; and 72°C for 10 min. The *TfGAPDH* (glyceraldehyde-3-phosphate dehydrogenase) was used as an internal control (Okuda *et al.*, 2009). The RT-PCR products were visualized by 1% agarose gel electrophoresis with Goldview™. Bands of 720 bp for *TfAOC* and 350 bp for *TfGAPDH* were obtained as predicted from the template sequences. The relative intensity of the signals was determined with LabImage 2.7.1 software and the ratio (*AOC*/*GAPDH*) was used for expressing the relative level of the mRNA expression.

Analysis of MeJA level: The endogenous content of MeJA from different organs (roots, stems, leaves, flowers) and tissues (pistils and anthers) were analyzed with the enzyme linked immunosorbent assay (ELISA) technique. The ELISA kit had previously been validated by HPLC and GC-MS analysis (Deng *et al.*, 2008). Samples were collected at 0 °C, immediately frozen in liquid nitrogen, and stored at -80 °C. Extraction, purification, and determination of endogenous MeJA were performed following the kit instructions. All samples were tested in three independent experiments with three replicates per experiment.

Results

Cloning and comparison of the full-length cDNA and genomic DNA sequence of *TfAOC*: Using the degenerate primers TfAOC3-1 and TfAOC3-2, a band of 560bp was specifically amplified. Sequence analysis showed it was highly homologous to AOCs from other plant species. Two pairs of primers were designed for 5′-RACE based on the obtained 3′-end sequence, and the full-length cDNA of *TfAOC* (GenBank accession no. JF417978) was obtained, which was subsequently confirmed by cycle sequencing. The cDNA was 954 bp long and contained a 723 bp ORF encoding 240 amino acids (Fig. 1A). A 5′-untranslated region of 49 bp was located upstream from the start codon with ATG as the transcript start, and a 3′-untranslated region of 182 bp was present downstream from the stop codon consisting of a poly (A) tail.

PCR amplification of the genomic DNA resulted in a distinct band of 1,212 bp. Comparison with the cDNA showed that the genomic DNA and cDNA matched base-to-base except that the genomic DNA contained two introns (Fig. 1B). The lengths of the two introns were 83 and 175 bp, respectively.

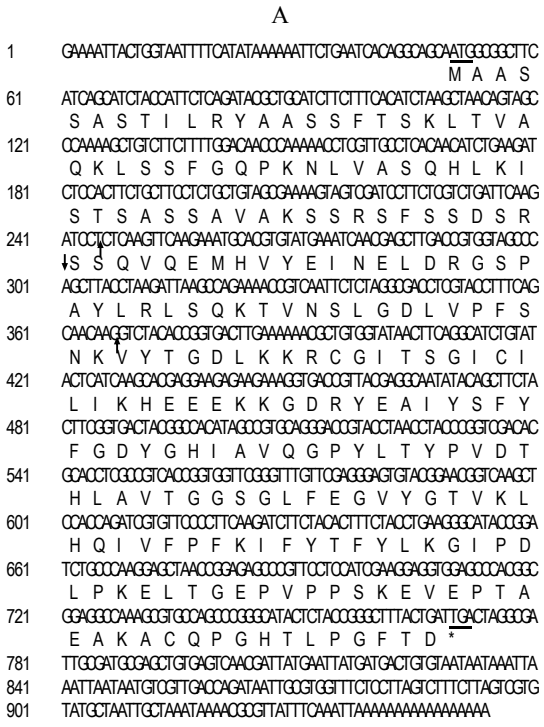

Fig. 1. Sequence analysis of the allene oxide cyclase gene from *T. fournieri*.
(A) Full-length cDNA sequence and deduced amino acid sequence. The start codon (ATG) and the stop codon (TGA) are underlined. A downward-pointing arrow indicates the cleavage site of the deduced chloroplast transit peptide between R64 and S65. (B) Intron 1 and intron 2 sequences. Intron 1 was located between nucleotides 245 and 246 and intron 2 was located between nucleotides 367 and 368. Upward-pointing arrows indicate the position of the introns.

Evolution of the deduced TfAOC protein and its biochemical characterization: A BlastP search of NCBI databases and the sequence alignment indicated the TfAOC protein showed high homology with other plant AOCs (Fig. 2). The TfAOC protein showed 72%, 71%, 67%, 67%, 66% and 66% identities to those of *Petunia ×hybrida* (ACD12705), *Nicotiana tabacum* (CAC33765), *Camellia sinensis* (ADY38579), *Camptotheca acuminata* (AAX56078), *Ipomoea nil* (ABC40984), and *Solanum lycopersicum* (AAK62358), respectively. In addition, molecular evolution analysis of the phylogenetic tree representing relationships among AOC proteins from different flowering plant species indicated that TfAOC was similar to proteins from Solanaceous species (Fig. 3).

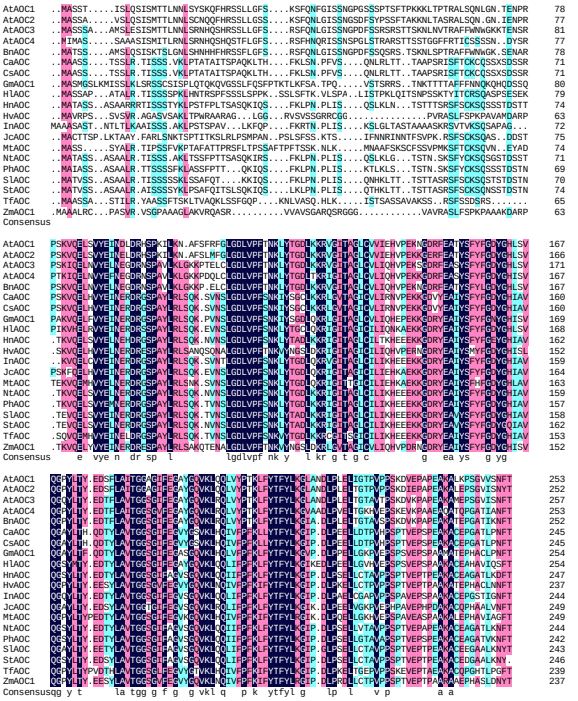

Fig. 2. Multiple alignment of the deduced amino acid sequence of TfAOC and AOC proteins from other plant species.
Amino acid sequences aligned were as follows: TfAOC, AtAOC1 (*Arabidopsis thaliana*, NP_189204), AtAOC2 (*A. thaliana*, NP_566776), AtAOC3 (*A. thaliana*, NP_566777), AtAOC4 (*A. thaliana*, NP_172786), BnAOC (*Brassica napus*, CY74379), CaAOC (*Camptotheca acuminata*, AAX56078), CsAOC (*Camellia sinensis*, ADY38579), GmAOC1 (*Glycine max*, AEE99196), HlAOCC1 (*Humulus lupulus*, AAT96851), HnAOC (*Hyoscyamus niger*, AAU11327), HvAOC (*Hordeum vulgare* subsp. *vulgare*, CAC83766), InAOC (*Ipomoea nil*, ABC40984), JcAOC (*Jatropha curcas*, ACZ06580), MtAOC (*Medicago truncatula*, CAI29046), NtAOC (*Nicotiana tabacum*, CAC83765), PhAOC (*Petunia ×hybrida*, ACD12705), SlAOC (*Solanum lycopersicum*, AAK62358), StAOC (*S. tuberosum*, AAN37418), ZmAOC1 (*Zea mays*, NP_001105245). Highly conserved residues are highlighted in black boxes, partially conserved residues in pink boxes, and the weakly similar residues in blue boxes.

The tree was constructed with MEGA 5.0 using the neighbor-joining method. The AOCs for analysis were indicated in Fig. 2. The numbers at each node represent percentage bootstrap support values for 1000 replicates.

Using the pI/Mw software tool, the pI and molecular weight of the deduced TfAOC protein were predicted to be 8.60 and 26.16 kDa, respectively. The AOC protein was rich in Ser residues at the N-terminus (26% for the first 50 amino acids), which is a common feature of chloroplast signal peptides. The Met was followed by an Ala residue and no charged amino acid was present among the first 10 amino acids. *In silico* analysis of the first 100 amino acids was performed with the TargetP 1.1 and ChloroP 1.1 programs; in both analyses chloroplast localization was predicted (cTP 0.890). The putative chloroplast signal peptide corresponds to the first 64 amino acids. The predicted pI and molecular weight without the putative chloroplast signal peptide were calculated to be 5.86 and 19.55, respectively.

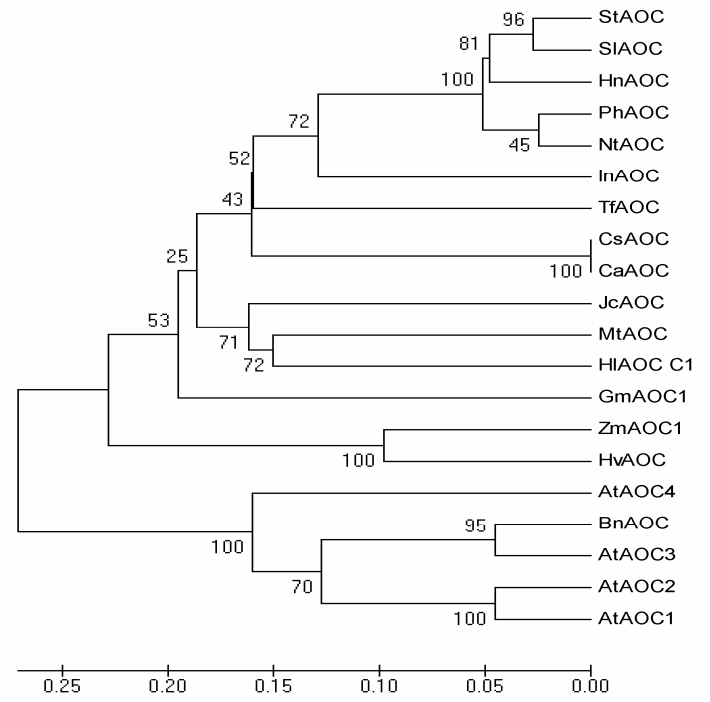

Fig. 3. Phylogenetic relationship of TfAOC and AOC proteins from other plant species.

Structure of the deduced TfAOC protein: Prediction of the TfAOC protein secondary structure was performed using the SOMPA program (Fig. 4A). Hierarchical neural network analysis revealed that the TfAOC protein was composed of 25.83% α-helix, 22.92% extended strand, 5.42% β-turn, and 45.83% random coil. The α-helix, extended strand and random coil constituted interlaced domination of the main part of the secondary structure.

The homology-based three-dimensional (3-D) structure of the TfAOC protein was modeled with the Swiss-Model program (Fig. 4B). TfAOC showed 64% sequence identity with AtAOC2 and the 3-D model of TfAOC was based on the temple 2brjB (X-Ray structure of AtAOC2). The 3-D model of TfAOC was predicted to form nine β-strands of the barrel, which are labeled S1–S9 (Fig. 4B). Similar to AtAOC2, TfAOC was hypothesized to be trimeric in crystals.

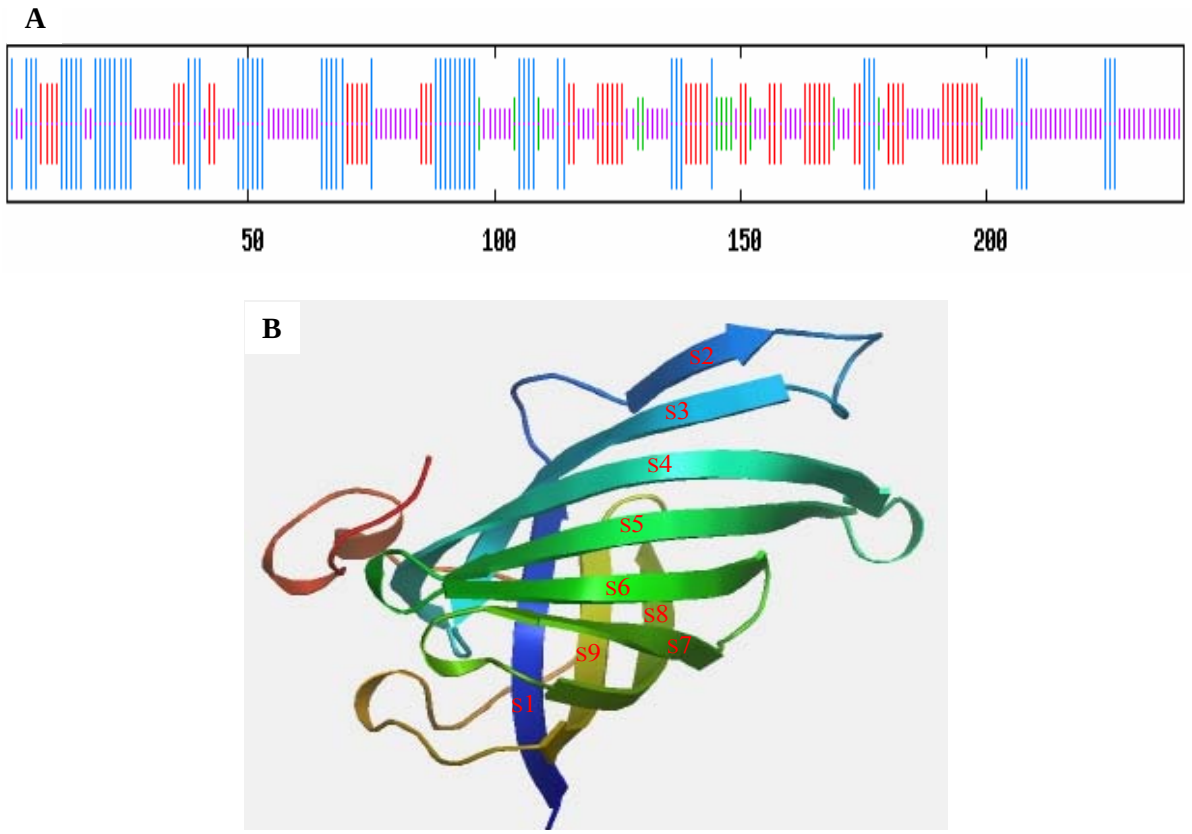

Fig. 4. Secondary and three-dimensional structures of the deduced TfAOC protein.
(A) Secondary structure of TfAOC protein. α-helix and extended strand are denoted as vertical long bars and vertical short bars, respectively. (B) Three-dimensional structure of TfAOC protein (predicted with Swiss-Model; http://cn.expasy.org). The β-strands of the barrel are labeled *S1*-*S9*.

Tissue-specific expression of *TfAOC*: Total RNAs extracted from different organs were analyzed by RT-PCR to investigate the *TfAOC* expression pattern. *TfAOC* was expressed in a constitutive manner and at different levels in the organs examined (Fig. 5A). The expression level of *TfAOC* in roots was lower than that in stems, leaves and flowers. The expression of *TfAOC* was high in pistil in the early flower buds and decreased in the latter development stage (Fig. 5A). Also, the expression of *TfAOC* was high in anthers.

Level of MeJA: The endogenous content of MeJA was detected with the MeJA ELISA kit. The level of MeJA was correlating with the expression levels of *TfAOC* (Fig. 5). The level of MeJA was lowest in roots and highest in leaves, the level of MeJA in flowers and stems was similar (Fig. 5B). There was higher MeJA level in the early development of the pistil during flower development and anthers showed higher level of MeJA than pistils (Fig. 5B).

Discussion

JA as a key signal molecule plays roles in series of developmental events (Wasternack, 2007; Browse, 2009). It has been known that the step that generates the correct precursor of JA biosynthesis is carried out by the enzyme AOC (Ziegler *et al.*, 2000; Hofmann *et al.*, 2006; Wasternack, 2007). In the moss *Physcomitrella patens*, *AOC* knock-out mutants showed reduced fertility (Stumpe *et al.*, 2010), indicating that AOC is also important for reproductive development.

Although *T. fournieri* is an ideal model plant for studying fertilization events, information on AOC in *T. fournieri* is still scant. *AOC* mRNA has been cloned from tomato (Ziegler *et al.*, 2000), *Arabidopsis* (Stenzel *et al.*, 2003b), barley (Maucher *et al.*, 2004), hop (Forts *et al.*, 2005), and *H. niger* (Jiang *et al.*, 2008). It was found that, most *AOC* mRNAs, except that from the moss *P. patens*, contained the chloroplast signal peptide (Stumpe *et al.*, 2010). In *T. fournieri*, signal peptide analysis demonstrated that TfAOC also shared characteristics with chloroplast signal peptides (Fig. 1) and hence chloroplast localization of TfAOC is suggested. Except for the signal peptide, the TfAOC amino acid sequence was highly conserved compared to several AOCs, especially the LGDLVPF sequence (Fig. 2). These conserved residues might be essential to maintain the correct functional structure of AOC (Hofmann *et al.*, 2006). AOC protein was first purified from corn seeds and characterized as a soluble and dimeric protein (Ziegler *et al.*, 1997), whereas the AOC2 protein from *Arabidopsis* was shown to be trimeric by crystallization (Hofmann *et al.*, 2006). TfAOC was presumed to be trimeric in crystals due to its high similarity in structure with AtAOC2, and thus they might have similar functions too.

Most *AOC* mRNAs are expressed constitutively in healthy plants and accumulated in response to wounding (Ziegler *et al.*, 2000; Stenzel *et al.*, 2003a; Jiang *et al.*, 2008). Adapting to its function in defense response, *AOC* mRNA is expressed most preferentially in vascular bundles (Hause *et al.*, 2000, 2003a, 2003b; Maucher *et al.*, 2004; Forts *et al.*, 2005; Cenzano *et al.*, 2007; Tretner *et al.* 2008; Kong *et al.*, 2009). However, the expression profile varied slightly in different plant species. For example, *AOC* was expressed mostly in leaves of *C. acuminata* (Pi *et al.*, 2008) and *Jatropha curcas* (Liu *et al.*, 2010), while the highest expression was found in flowers of tomato (Hause *et al.*, 2000), *Arabidopsis* (Hause *et al.*, 2003b) and *Artemisia annua* (Lu *et al.*, 2011). Our RT-PCR results showed that *TfAOC* mRNA was expressed highly in leaves, flowers and stems but relatively lower in roots (Fig. 5A). The tissue expression profile of *TfAOC* was well in line with that observed in other plant species.

The *Arabidopsis* mutants in JA biosynthesis or perception were male sterile, with abnormal or not mature pollen, delayed or defected anther dehiscence (Feys *et al.*, 1994; McConn & Browse, 1996; Sanders *et al.*, 2000; Ishiguro *et al.*, 2001; von Malek *et al.*, 2002), revealing that JA was required for anther development in *Arabidopsis*. In this work, high expression of *AOC* mRNA in anthers suggested that JA was also required for anther development in *T. fournieri* (Fig. 5A). However, JA-insensitive tomato mutant was female sterile (Li *et al.*, 2001; 2004), and the representation of LOX, AOC and a pistil-specific JA methyltransferase supported the involvement of JA in development of female reproductive organ in tobacco (Avanci *et al*., 2010). These studies strongly supported the role of JA in the female reproductive development in Solanaceous species. In our study, *AOC* mRNA expressed in the pistils and showed higher expression level in the early development stage, suggesting that JA was involved in the female reproductive development of *T. fournieri* (Fig. 5A). The molecular evolution analysis showed that TfAOC was similar to proteins from Solanaceous species and the result supports the point that JA may play a role in pistil development. *TfAOC* mRNA was expressed highly in pistils and anthers, in agreement with the study that *AOC* mRNA expressed specifically in flowers of transgenic tomato and tobacco (Stenzel *et al.*, 2008).

In addition, there is a correlation between the JA level and the expression of *AOC* mRNA. In tomato, the high levels of *AOC* mRNA and AOC protein in different flower organs correlate with high AOC activity, and with elevated levels of JA, OPDA and JA isoleucine conjugate (Hause *et al.* 2000). When the *Pharbitis nil* was treated with theobroxide (structurally similar with JA), the expression pattern of *AOC* mRNA was increased (Kong *et al.* 2009). In the present study, the change of MeJA level was also consistent with that of the *AOC* mRNA expression, further suggesting that JA might be essential in reproductive development in *T. fournieri*.

Although JA was demonstrated to be important for male fertility in *Arabidopsis* and female fertility in tomato. *AOC* is required for moss fertility in previous studies, the role of JA in *T. fournieri* remains an interesting question to be addressed. In our study, *AOC* was highly expressed in reproductive organs and the MeJA content was consistent with *AOC* expression level. These results suggested JA was involved in anther and pistil development. Considering *T. fournieri* is a model plant for study of female development, a full characterization and tissue expression of *AOC* we present here will be useful to study the role of JA in *T. fournieri* in the future.

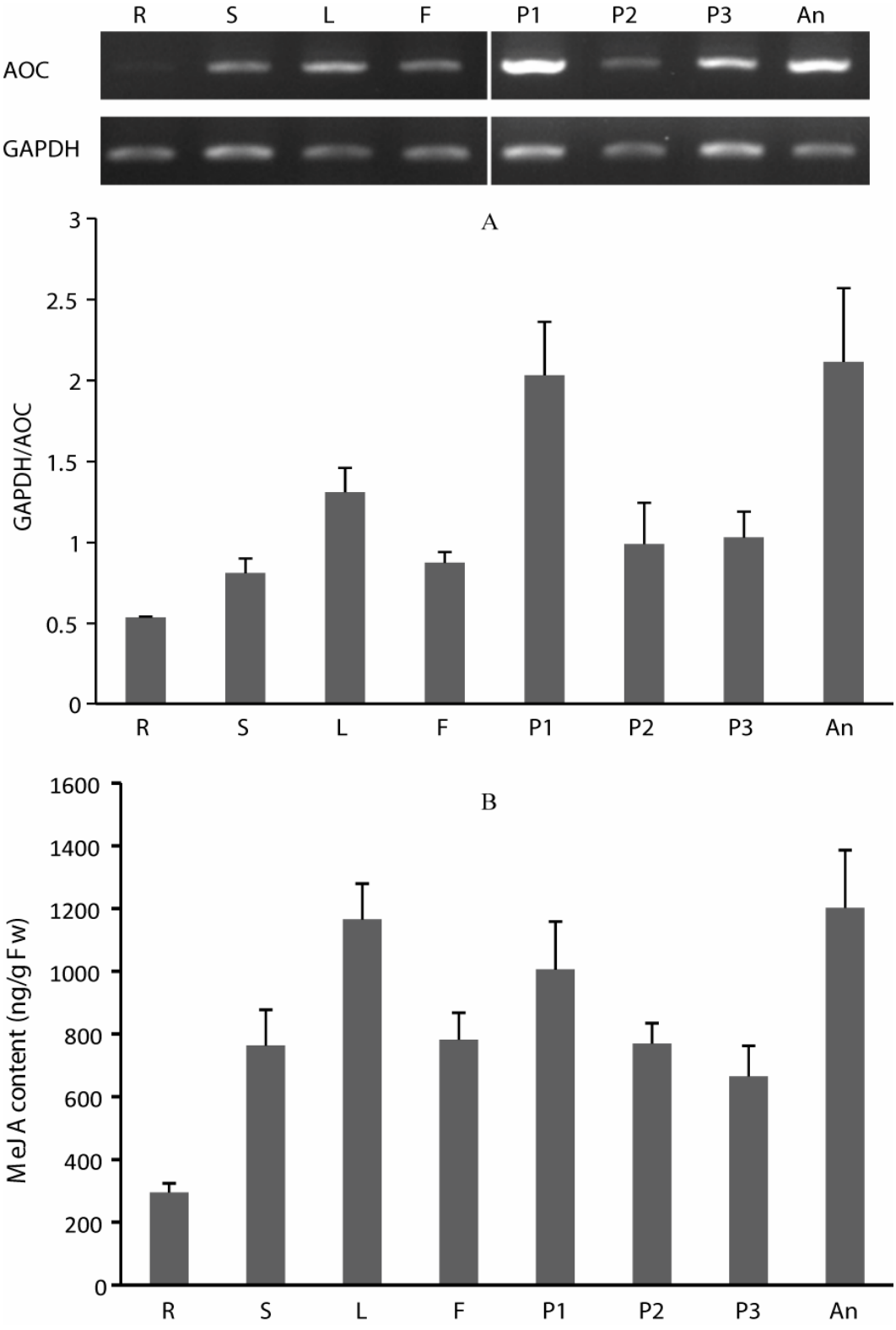

Fig. 5. Expression of *TfAOC* mRNA is correlated with the level of MeJA in *T. fournieri*.
(A) Expression profile of *TfAOC* mRNA. Total RNA was isolated from roots (R), stems (S), leaves (L), flowers (F), pistils at two-nucleate stage (P1), pistils at seven-celled stage before flower opening (P2), pistils of opening flowers (P3) and anthers (An). The *TfGAPDH* gene was chosen as an internal control. The relative mRNA expression was performed with LabImage 2.7.1 software. (B) The content of MeJA in different organs/tissues. The isolation, purification and determination of MeJA were carried out with the ELISA kit. The data represents the means ± SD (standard deviation) from three independent experiments.

Acknowledgments

We are grateful to Prof. Jun-Xian He for his critical reading of the manuscript. This work was supported by a grant from the Natural Science Foundation of Guangdong Province (no. 003062).

References

Aida, R., S. Kishimoto, Y. Tanaka and M. Shibata. 2000. Modification of flowers color in torenia (*Torenia fournieri* Lind.) by genetic transformation. *Plant Sci.*, 153: 33-42.

Arnold, K., L. Bordoli, J. Kopp and T. Schwede. 2006. The SWISS-MODEL workspace: a web-based environment for protein structure homology modelling. *Bioinformatics*, 22: 195-201.

Avanci, N.C., D.D. Luche, G.H. Goldman and M.H.S. Goldman. 2010. Jasmonates are phytohormones with multiple functions, including plant defense and reproduction. *Genet. Mol. Res.*, 9(1): 484-505.

Bjellqvist, B., G.J. Hughes, Ch. Pasquali, N. Paquet, F. Ravier, J. Ch. Sanchez, S. Frutiger and D.F. Hochstrasser. 1993. The focusing positions of polypeptides in immobilized pH gradients can be predicted from their amino acid sequences. *Electrophoresis*, 14: 1023-1031.

Browse, J. 2009. Jasmonate passes muster: a receptor and targets for the defense hormone. *Annu. Rev. Plant Biol.*, 6: 183-205.

Cenzano, A., G. Abdala and B. Hause. 2007. Cytochemical immuno-localization of allene oxide cyclase, a jasmonic acid biosynthetic enzyme, in developing potato stolons. *J. Plant Physiol.*, 164(11): 1449-1456.

Combet, C., C. Blanchet, C. Geourjon and G. Deléage. 2000. NPS@: network protein sequence analysis. *Trends Biochem. Sci.*, 25(3): 147-150.

Deng, A., W. Tan, S. He, W. Liu, T. Nan, Z. Li, B. Wang and Q.X. Li. 2008. Monoclonal antibody-based enzyme linked immunosorbent assay for the analysis of jasmonates in plants. *J. Integr. Plant Biol.*, 50(8): 1046-1052.

Emanuelsson, O., H. Nielsen and G. von Heijne. 1999. ChloroP, a neural network-based method for predicting chloroplast transit peptides and their cleavage sites. *Protein Sci.*, 8(5): 978-984.

Emanuelsson, O., H. Nielsen, S. Brunak and G. von Heijne. 2000. Predicting subcellular localization of proteins based on their N-terminal amino acid sequence. *J. Mol. Biol.*, 300: 1005-1016.

Feys, B.J.F, C.E. Benedetti, C.N. Penfold and J.G. Turner. 1994. *Arabidopsis* mutants selected for resistance to the phytotoxin coronatine are male sterile, insensitive to jasmonate, and resistant to a bacterial pathogen. *Plant Cell*, 6:751-759.

Fortes, A.M., O. Miersch, P.R . Lange, R. Malhó, P.S. Testillano, Mdel. C. Risueño, C. Wasternack and M.S. Pais. 2005. Expression of allene oxide cyclase and accumulation of jasmonates during organogenic nodule formation from hop (*Humulus lupulus* var. Nugget) internodes. *Plant Cell Physiol.*, 46(10):1713-1723.

Hause, B., G. Hause, C. Kutter, O. Miersch and C. Wasternack. 2003a. Enzymes of jasmonate biosynthesis occur in tomato sieve elements. *Plant Cell Physiol.*, 44(6): 643-648.

Hause, B., I. Stenzel, O. Miersch and C. Wasternack. 2003b. Occurrence of the allene oxide cyclase in different organs and tissues of *Arabidopsis thaliana*. *Phytochemistry*, 64(5): 971-980.

Hause, B., I. Stenzel, O. Miersch, H. Maucher, R. Kramell, J. Ziegler and C. Wasternack. 2000. Tissue-specific oxylipin signature of tomato flowers: allene oxide cyclase is highly expressed in distinct flower organs and vascular bundles. *Plant J.*, 24(1): 113-126.

Higashiyama, T., H. Kuroiwa and T. Kuroiwa. 2003. Pollen-tube guidance: beacons from the female gametophyte. *Curr. Opin. Plant Biol.*, 6: 36-41.

Higashiyama, T., H. Kuroiwa, S. Kawano and T. Kuroiwa. 1998. Guidance in vitro of the pollen tube to the naked embryo sac of *Torenia fournieri*. *Plant Cell*, 10: 2019-2031.

Hofmann, E., P. Zerbe, F. Schaller. 2006. The crystal structure of *Arabidopsis thaliana* allene oxide cyclase: insights into the oxylipin cyclization reaction. *Plant Cell*, 18(11): 3201-3217.

Imre, K. and Z. Kristof. 1999. Isolation and osmotic relations of developing megagametophytes of *Torenia fournieri*. *Sex Plant Reprod.*, 12: 152-157.

Ishiguro, S., A. Kawai-Oda, K. Ueda, I. Nishida and K. Okada. 2001. The Defective in Anther Dehiscence1 gene encodes a novel phospholipase A1 catalyzing the initial step of jasmonic acid biosynthesis, which synchronizes pollen maturation, anther dehiscence, and flower opening in *Arabidopsis*. *Plant Cell*, 13: 2191-2209.

Jiang, K., Z. Liao, Y. Pi, Z. Huang, R. Hou, Y. Cao, Q. Wang, Z. Sun and K. Tang. 2008. Molecular cloning and expression profile of a jasmonate biosynthetic pathway gene allene oxide cyclase from *Hyoscyamus niger*. *Mol. Biol.*, 42(3): 434-444.

Kong, F.J., Y. Li, J. Abe, B. Liu, F. Schaller, M. Piotrowski, S. Otagaki, K. Takahashi, H. Matsuura, T. Yoshihara and K. Nabeta. 2009. Expression of allene oxide cyclase from *Pharbitis nil* upon theobroxide treatment. *Biosci. Biotechnol. Biochem.*, 73(5): 1007-1013.

Li, L., C. Li and G.A. Howe. 2001. Genetic analysis of wound signaling in tomato. Evidence for a dual role of jasmonic acid in defense and female fertility. *Plant Physiol.*, 127: 1414-1417.

Li, L., Y. Zhao, B.C. McCaig, B.A. Wingerd, J. Wang, M.E. Whalon, E. Pichersky and G.A. Howe. 2004. The tomato homolog of CORNATINE-INSENSITIVE1 is required for the maternal control of seed matureation, jasmonate-signaled defense responses, and glandular trichome development. *Plant Cell*, 16: 126-143.

Liu, B., W. Wang, J. Gao, F. Chen, S. Wang, Y. Xu, L. Tang and Y. Jia. 2010. Molecular cloning and characterization of a jasmonate biosynthetic pathway gene for allene oxide cyclase from *Jatropha curcas*. *Acta. Physiol. Plant*, 32: 531-539.

Lu, X., X. Lin, Q. Shen, F. Zhang, Y. Wang, Y. Chen, T. Wang, S. Wu and K. Tang. 2011. Characterization of the jasmonate biosynthetic gene allene oxide cyclase in *Artemisia annua* L., source of the antimalarial drug artemisinin. *Plant Mol. Biol. Rep.*, 29: 489-497.

Maucher, H., I. Stenzel, O. Miersch, N. Stein, M. Prasad, U. Zierold, P. Schweizer, C. Dorer, B. Hause and C. Wasternack. 2004. The allene oxide cyclase of barley (*Hordeum vulgare* L.)-cloning and organ-specific expression. *Phytochemistry*, 65(7): 801-811.

McConn, M. and J. Browse. 1996. The critical requirement for linolenic acid is pollen development, not photosynthesis, in an *Arabidopsis* mutant. *Plant Cell*, 8: 403-416.

Okuda, S., H. Tsutsui, K. Shiina, S. Sprunck, H. Takeuchi, R. Yui, R.D. Kasahara, Y. Hamamura, A. Mizukami, D. Susaki, N. Kawano and T. Sakakibara. 2009. Defensin-ike polypeptide LUREs are pollen tube attractants secreted from synergid cells. *Nature*, 458: 357-362.

Pi, Y., Z. Liao, K. Jiang, B. Huang, Z. Deng, D. Zhao, H. Zeng, X. Sun and K. Tang. 2008. Molecular cloning, characterization and expression of a jasmonate biosynthetic pathway gene encoding allene oxide cyclase from *Camptotheca acuminata*. *Biosci. Rep.*, 28(6): 349-355.

Saitou, N. and M. Nei. 1987. The neighbor-joining method: a new method for reconstructing phylogenetic trees. *Mol. Biol. Evol.*, 4: 406-425.

Sanders, P.M., P.Y. Lee, C. Biesgen, J.D. Boone, T.P. Beals, E.W. Weiler, R.B. Goldberg. 2000. The *Arabidopsis* DELAYED DEHISCENCE1 gene encodes an enzyme in the jasmonic acid synthesis pathway. *Plant Cell*, 12: 1041-1062.

Stenzel, I., B. Hause, H. Maucher, A. Pitzschke, O. Miersch, J. Ziegler, C.A. Ryan and C. Wasternack . 2003a. Allene oxide cyclase dependence of the wound response and vascular bundle-specific generation of jasmonates in tomato - amplification in wound signalling. *Plant J.*, 33(3): 577-589.

Stenzel, I., B. Hause, R. Proels, O. Miersch, M. Oka, T. Roitsch and C. Wasternack. 2008. The AOC promoter of tomato is regulated by developmental and environmental stimuli. *Phytochemistry*, 69: 1859-1869.

Stenzel, I., B. Hause, R. Proels, O. Miersch, T. Kurz, M. Maucher, H. Weichert, J. Ziegler, I. Feussner and C. Wasternack. 2003b. Jasmonate biosynthesis and the allene oxide cyclase family of *Arabidopsis thaliana*. *Plant Mol. Bio.*, 51: 895-911.

Stumpe, M., C. Göbel, B. Faltin, A.K. Beike, B. Hause, K. Himmelsbach, J. Bode, R. Kramell, C. Wasternack, W. Frank, R. Reski and I. Feussner. 2010. The moss *Physcomitrella patens* contains cyclopentenones but no jasmonates: mutations in allene oxide cyclase lead to reduced fertility and altered sporophyte morphology. *New Phytol.*, 188(3): 740-749.

Tretner, C., U. Huth and B. Hause. 2008. Mechanostimulation of *Medicago truncatula* leads to enhanced levels of jasmonic acid. *J. Exp. Bot.*, 59(10): 2847-2856.

von Malek, B., E. van der Graaff, K. Schneitz, B. Keller. 2002. The *Arabidopsis* male-sterile mutant *dde2-2* is defective in the ALLENE OXIDE SYNTHASE gene encoding one of the key enzymes of the jasmonic acid biosynthesis pathway. *Planta*, 216: 187-192.

Wasternack, C. 2007. Jasmonates: an update on biosynthesis, signal transduction and action in plant stress response, growth and development. *Ann. Bot.*, 100 (4): 681-697.

Ziegler, J., I. Stenzel, B. Hause, H. Maucher, M. Hamberg, R. Grimm, M. Ganal and C. Wasternack. 2000. Molecular cloning of allene oxide cyclase. The enzyme establishing the stereochemistry of octadecanoids and jasmonates. *J. Biol. Chem.*, 275(25): 19132-19138.

Ziegler, J., M. Hamberg, O. Miersch and B. Parthier. 1997. Purification and characterization of allene oxide cyclase from dry corn seeds. *Plant Physiol.*, 114(2): 565-573.

(Received for publication 15 May 2011)